Simulation and Theory of Ions at Atmospherically Relevant Aqueous Liquid-Air Interfaces

Douglas J. Tobias,[1] Abraham C. Stern,[1]
Marcel D. Baer,[2] Yan Levin,[3]
and Christopher J. Mundy[2]

[1]Department of Chemistry, University of California, Irvine, California 92697-2025; email: dtobias@uci.edu, acstern@uci.edu

[2]Chemical and Materials Science Division, Pacific Northwest National Laboratory, Richland, Washington 99352; email: marcel.baer@pnnl.gov, chris.mundy@pnnl.gov

[3]Insituto de Física, Universidade Federal do Rio Grande do Sul, CEP 91501-970 Porto Alegre, RS, Brazil; email: levin@if.ufrgs.br

Annu. Rev. Phys. Chem. 2013. 64:339–59

First published online as a Review in Advance on January 16, 2013

The *Annual Review of Physical Chemistry* is online at physchem.annualreviews.org

This article's doi:
10.1146/annurev-physchem-040412-110049

Keywords

atmospheric chemistry, interfacial chemistry, specific ion effects, molecular dynamics, dielectric continuum theory

Abstract

Chemistry occurring at or near the surface of aqueous droplets and thin films in the atmosphere influences air quality and climate. Molecular dynamics simulations are becoming increasingly useful for gaining atomic-scale insight into the structure and reactivity of aqueous interfaces in the atmosphere. Here we review simulation studies of atmospherically relevant aqueous liquid-air interfaces, with an emphasis on ions that play important roles in the chemistry of atmospheric aerosols. In addition to surveying results from simulation studies, we discuss challenges to the refinement and experimental validation of the methodology for simulating ion adsorption to the air-water interface and recent advances in elucidating the driving forces for adsorption. We also review the recent development of a dielectric continuum theory capable of reproducing simulation and experimental data on ion behavior at aqueous interfaces.

1. INTRODUCTION

Aerosol: stable suspension of particles in the atmosphere

MD: molecular dynamics

DCT: dielectric continuum theory

Aqueous liquid-air interfaces are ubiquitous in the atmosphere. Common examples include the surfaces of cloud droplets, aqueous aerosols, thin films of water on boundary-layer surfaces (soils, plant, buildings, etc.), and the quasi-liquid layer on ice and snow. These aqueous environments contain myriad chemical species dissolved within them or adsorbed on their surfaces, such as inorganic atomic and molecular ions, acids and bases, and a wide variety of organic compounds. Chemical reactions occurring in these environments are involved in both the formation and removal of trace gases in the atmosphere and hence contribute to the determination of air quality. The chemistry of aerosol particles modifies their optical properties and potency as cloud condensation nuclei and therefore is relevant to radiative forcing and climate.

During the past 20 years, it has become increasingly apparent that many important atmospheric chemical processes occur at aqueous-air interfaces (1–6). Examples of such heterogeneous chemical processes include the hydrolysis of SO_2 in cloud droplets, which is involved in the production of acid rain (7); the oxidation of Cl^- to Cl_2 in sea-salt aerosol, which contributes to ozone formation in the polluted marine boundary layer (2, 8); and the destruction of tropospheric ozone via halogen chemistry in the Arctic (9). It is also becoming increasingly clear that the aqueous liquid-air interface provides a unique setting that enables chemistry that does not occur or is too slow to be relevant in bulk solution (2, 10).

The experimental determination of the kinetics and mechanisms of interfacial chemical processes is particularly challenging because of the inherent difficulty in making measurements that provide a molecular-scale view of the composition, structure, dynamics, and chemistry at liquid interfaces. Consequently, much recent progress in the molecular-scale understanding of heterogeneous atmospheric chemistry has come from molecular dynamics (MD) simulation studies, often carried out in close collaboration with laboratory studies. In addition to providing insight into particular chemical processes relevant to atmospheric chemistry, MD simulations have also contributed to the development of fundamental theoretical concepts that are broadly applicable to a wide variety of problems in interfacial chemistry and are guiding the refinement of theories of aqueous solutions, such as dielectric continuum theory (DCT).

In this review, we present and discuss recent simulation studies and developments in DCT that are relevant to the heterogeneous atmospheric chemistry of aqueous ionic solutions in the environment. This is a large and rapidly growing area of research that cannot be covered completely here. We have chosen, therefore, to restrict our focus to the behavior of inorganic ions, with an emphasis on halide anions, at the air-water interface. For a more complete picture, we refer the reader to other recent reviews that present complementary perspectives (10–13).

2. HALIDE IONS: CONSENSUS VIEW FROM SIMULATION AND EXPERIMENT

Marine aerosols formed by bursting bubbles in seawater contain halide anions (Cl^-, Br^-, and I^-), which participate in numerous reactions with atmospheric trace gases, and it is now clear that some of the rich halide chemistry occurs on the surface of sea-salt aerosol particles or snow on which sea salt has been deposited (9, 10, 14). A prerequisite for an interfacial reaction is that the reactants (i.e., ions) must be present at the interface. Until approximately 20 years ago, this seemed paradoxical because the conventional wisdom, discussed in more detail below, was that ions are repelled from the air-water interface. However, in the early 1990s, MD simulations employing polarizable force fields (FFs) predicted that the heavier halides prefer to be located on the surface of water clusters (15–21), and in the early 2000s, simulations of alkali halide solutions with extended interfaces,

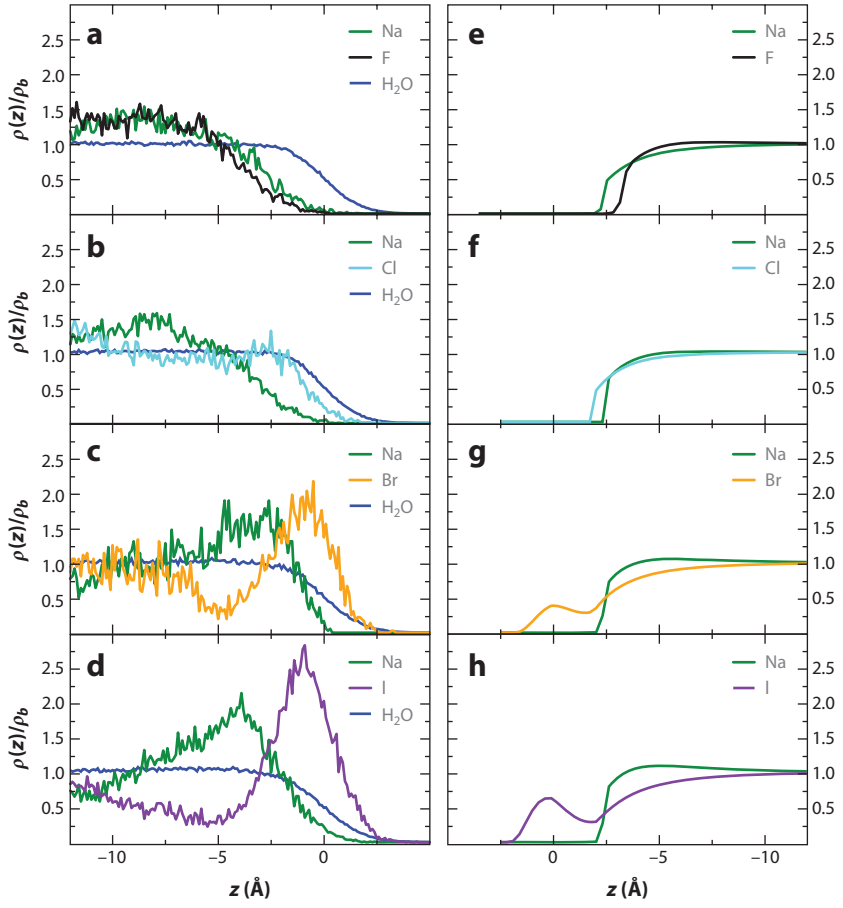

Figure 1

Ion density profiles in 1-M sodium halide solutions from (*a–d*) molecular dynamics (MD) simulations with polarizable force fields (22) and (*e–h*) the polarizable anion dielectric continuum theory (PA-DCT) (37). In panels *a–d*, the water density profiles are drawn in blue. The density profiles are normalized by the bulk densities and plotted as a function of the distance from the air-water interface, defined as the Gibbs dividing surface, located at $z = 0$. MD simulations and the PA-DCT provide the same qualitative picture of anion adsorption to the air-water interface, namely that large polarizable anions can be present at the air-water interface, but the extent of anion adsorption predicted by the PA-DCT is substantially less than that predicted by the MD simulations.

modeled as slabs subjected to periodic boundary conditions, and employing similar FFs, predicted that the heavier halides can adsorb to the solution-air interface, with an adsorption propensity that follows the order $Cl^- < Br^- < I^-$ (22–25) (**Figure 1**). These simulations inspired many new experimental investigations, the earliest of which included second harmonic generation (SHG) (26–28), vibrational sum-frequency generation (VSFG) (29, 30), and photoelectron spectroscopy (PES) (31, 32) measurements, that essentially validated the predictions of the simulations. For reviews of the early simulations of halide ion adsorption and their experimental validation, readers are referred to References 11 and 33–36.

SHG: second harmonic generation

VSFG: vibrational sum-frequency generation

PES: photoelectron spectroscopy

3. MODEL DEPENDENCE OF SIMULATION RESULTS

PMF: potential of mean force

Gibbs dividing surface (GDS): position in interface at which the surface excess of solvent is zero

During the past decade, there has been explosive growth in the number of simulation studies of halide ion adsorption to the air-water interface. The majority of these studies fall roughly into two categories: (*a*) those that focus on intrinsic adsorption propensities via calculation of the potential of mean force (PMF) for single-ion adsorption in the absence of counterions and (*b*) simulations of halide salt solutions at finite concentration. The growing body of recent work has exposed a significant level of model dependence of halide ion–adsorption propensity. Nonetheless, there is general agreement on the order of this propensity, that alkali cations and fluoride anions are repelled from the interface, and that iodide anions adsorb, although, as discussed below, the extent of the adsorption of the heavier halides (Br^- and I^-) is model dependent.

The empirical potential energy functions or FFs that describe interatomic interactions in aqueous ionic solutions contain terms that describe hard-core repulsive and attractive dispersion interactions, typically modeled using Lennard-Jones potentials, and coulomb interactions between fixed charges on the ions and water molecules. Ion electronic polarization is typically accounted for explicitly by induced dipoles (15–19, 24, 38) or Drude oscillators (20, 21, 39, 40), in which the atomic polarizabilities are key parameters. Various target data have been used to optimize FF parameters for ions, including quantum chemical calculations on ion-water complexes, and the structural and thermodynamic properties of bulk electrolytes (24, 38, 41). Water models are generally not optimized for ion-water interactions; hence the resulting ion parameters are tied closely to the water model with which they are meant to be used. As emphasized in the recent literature, the parameterization of the halide anions is underdetermined, in the sense that there are degenerate sets of parameters that reproduce available target data equally well (13, 41, 42). Interfacial properties are not generally considered as target data. It is not surprising, therefore, that there is a wide range of variability in the extent of halide adsorption predicted by different models.

Ion adsorption propensity, quantified in terms of single-ion PMFs, varies substantially among the different FFs found in the literature. PMFs that display minima near the Gibbs dividing surface (GDS) imply that ion adsorption is favorable thermodynamically and that the density or concentration of the ion is greater at the interface than in the bulk. Nonpolarizable FFs typically predict that, among the halides, only iodide is stabilized at the interface (by $\approx$0.5 kcal mol^{-1}) and that the lighter halides, although not stabilized at the interface, are able to approach it more closely in the order $F^- < Cl^- < Br^-$ (see, e.g., 42). Polarizable FFs tend to predict the same order of closeness of approach and that, in addition to I^-, Br^- is also stabilized at the interface (see, e.g., 24, in which single-ion PMFs show that Br^- is stabilized by $\approx$1 kcal mol^{-1} and I^- by $\approx$1.5 kcal mol^{-1}).

Whereas systematic variation of FF parameters, such as charge, radius, and polarizability, is useful for elucidating interactions that contribute to ion adsorption (42–45), for making predictions that are useful for understanding heterogeneous atmospheric chemistry, accuracy, as judged by direct comparison to experimental data, is desirable. How well do the disparate halide FFs perform? The answer to this question depends, unfortunately, on the data used for comparison.

4. ISSUES CONCERNING EXPERIMENTAL VALIDATION

The surface tensions of inorganic salt solutions increase with concentration (46, 47). Surface-tension data for halide salts are available over a wide range of concentrations, but surface tensions derived from MD simulations are difficult to converge (48, 49). Dos Santos et al. (48) compared surface tensions from MD simulations based on two nonpolarizable potentials to experimental data for NaF and NaI and noted only mediocre agreement. For NaI at low concentrations, they found that the surface tension was lower than that of neat water, in stark contrast to experimental

data. D'Auria & Tobias (49) computed surface tensions for 1-m and 6-m KF and NaCl solutions using both polarizable and nonpolarizable FFs and found a similar, mediocre level of agreement with experimental data. Netz and colleagues (42, 50) used single-ion PMFs in extended Poisson-Boltzmann (PB) calculations of ion concentration profiles, from which surface tensions were derived. Generally speaking, they found that nonpolarizable FFs optimized for solution thermodynamic data led to better agreement with experimental surface-tension data than a polarizable FF did. When comparing PB calculations to experimental data, we note that the PB calculations appear to underestimate the extent of ion adsorption (and hence are expected to overestimate the surface tensions) compared to MD simulations for a given FF, at least for 0.85-M NaBr and NaI (42).

Poisson-Boltzmann (PB) theory: mean field theory for ion distributions derived by combining Poisson's equation with the Boltzmann distribution

VSFG is a surface-sensitive, nonlinear vibrational spectroscopic technique that has been used extensively to probe solute-induced changes in water hydrogen bonding at aqueous interfaces (33, 51, 52). VSFG spectra of NaF and NaCl solutions are very similar to the spectrum of neat water, suggesting that F^- and Cl^- do not perturb the water surface (29, 30). Conversely, the spectra of NaBr and NaI solutions exhibit differences from the neat water spectrum (29, 30, 53), which have been attributed to the presence of the heavier halides in the interfacial region (29, 53). Accurate calculation of VSFG spectra from MD trajectories is challenging (54–58), but a reasonable level of agreement with experimental VSFG data has been achieved for NaCl and NaI solutions using a polarizable model that predicted strong adsorption of I^- (59, 60).

SHG is a second-order spectroscopic technique that probes electronic transitions in interfacial settings. It has been used to probe bromide and iodide ions at aqueous interfaces (28, 36, 61). To quantify ion adsorption propensities, one can fit the concentration dependence of the SHG response to a Langmuir adsorption isotherm, which affords an adsorption free energy, albeit typically with considerable uncertainty. Values for I^- range from -6.2 kcal mol^{-1} at low concentrations (0.1 M to 2 M) to -0.8 kcal mol^{-1} at higher concentrations (>2 M) (28, 36). For Br^-, the best fit to SHG data from 6 mM to 7 M gave an adsorption free energy of -0.3 kcal mol^{-1} (61). Thus, consistent with MD simulations employing polarizable FFs, analysis of SHG data suggests that both Br^- and I^- adsorb and that, for I^- at low concentration, the adsorption is much more favorable than single-ion PMFs suggest.

Recent advancements in PES experiments carried out at synchrotrons have enabled species-selective depth profiling of aqueous solutions (34, 62). Depth profiling is possible because as the incident photon energy is increased, electrons from deeper in the solution have sufficient kinetic energy to make it to the detector. Thus photoelectron kinetic energy (PKE) is a measure of the probing depth. Unfortunately, a precise relation between PKE and depth in spatial units is not available (63). Measurements of the anion/cation ratio as a function of PKE have been reported for highly concentrated alkali halide solutions. For KF solutions, the ratio is unity over a range of PKE probing, from near the solution surface to the bulk (64). At low PKE, which corresponds to the interfacial region, the ratio increases from 1.5 in NaCl to 2 in KBr to 4 in KI (32, 65). Interfacial anion/cation ratios derived from MD simulations with polarizable FFs compare quite favorably with those derived from the experimental PES data (63–66). MD simulations have proven useful for enhancing the interpretation of PES data. For example, the anion/cation ratios obtained for NaCl and RbBr from PES data and MD simulations suggested no difference in the ion distributions in both salt solutions, but the MD simulations with polarizable FFs predicted that the Cl^- interfacial propensity was greater in NaCl versus RbCl, and this prompted measurements of Cl^-/O distributions that confirmed the simulations' predictions (65).

X-ray reflectivity (XRR) measurements probe electron density inhomogeneities at interfaces, and models are required to extract electron density profiles of the individual species in a multicomponent system. Density profiles extracted from XRR data for concentrated chloride and iodide solutions suggested that these ions are depleted from the solution-air interface (67), in contrast to

predictions from MD simulations. Attempts have been made to reconcile MD simulations with XRR data via comparison of the structure factors rather than the model-dependent density profiles (68–70). These studies have been mostly inconclusive because of lack of quantitative agreement between the structure factors obtained experimentally and those computed from the MD trajectories. However, using a new polarizable FF, Dang et al. (70) recently were able to compute structure factors that were in satisfactory agreement with XRR data for $SrCl_2$, thereby establishing that the strong Cl^- interfacial enhancement observed in their simulation is not incompatible with XRR data.

Gibbs adsorption isotherm: equation relating the surface excess of a solute to the derivative of the surface tension with respect to solute concentration

Presently, on the whole, surface-tension data tend to favor nonpolarizable models of halide ions, whereas surface-sensitive spectroscopies tend to favor polarizable models. For progress in the validation of FFs used to model halide solutions, the little or no adsorption inferred from surface-tension data needs to be reconciled with the relatively strong adsorption implied by most available spectroscopic data. To this end, advances in methodology for calculating spectroscopic observables from MD simulations and more careful comparisons of simulations to spectroscopic data are required.

5. POLARIZABLE ANION DIELECTRIC CONTINUUM THEORY

DCT for electrolyte solutions has a long and venerable history. Almost a century ago, Debye & Hückel (71) developed the first simple DCT of bulk electrolytes. Within the Debye-Hückel (DH) theory, ions are treated as hard spheres with a fixed uniform surface charge q, and water is idealized as a continuum medium of dielectric constant ε_w. DH theory was the first to successfully account for the osmotic properties of bulk electrolytes and has served as the starting point for the development of more rigorous statistical mechanical theories of electrolyte solutions (72).

The development of a successful DCT of the electrolyte-air interface has proven to be difficult. The first observation that electrolytes affect the thermodynamics of the air-water interface appeared in the pioneering work of Heydweiller (46), who noted that the addition of a strong electrolyte to water leads to an increase of the surface tension of the air-water interface. An explanation of this phenomenon was advanced by Langmuir (73), who, appealing to the Gibbs adsorption isotherm, suggested (for reasons that were not very clear) that ions preferred to stay away from the interfacial region. The mechanism responsible for the ionic depletion from the interfacial region was elucidated by Wagner (74) and Onsager & Samaras (75). Using the DH-DCT, these authors suggested that as an ion approaches the GDS, it is repelled by its image charge located on the air side of the interface, and this repulsion drives ions away from the interfacial region. Using DH theory, Onsager & Samaras calculated the ion-image repulsion potential assuming zero ionic radius. Substituting this expression into the Gibbs adsorption isotherm, they were able to obtain a limiting law for the excess surface tensions of electrolyte solutions, which agreed quite well with the experimental data for dilute NaCl solutions. Onsager & Samaras also attempted to extend the range of validity of their expression for surface tension by including a finite ionic radius. To this end, they adopted the interionic interaction potential derived by Debye & Hückel for bulk electrolytes. This improved the value of the calculated surface tension, making it agree with experiments up to 100 mM. At higher concentrations, however, strong deviations from the experimental data appeared.

The problem of the surface tensions of electrolyte solutions was reexamined by Levin & Flores-Mena (76) at the turn of the previous century. They included two new components in the Onsager-Samaras theory of surface tension: (*a*) ionic hydration and (*b*) the polarizability of the counterion screening cloud surrounding each ion. Ionic hydration was assumed to prevent ions from coming closer to the GDS than their hydrated radius, whereas the broken translational symmetry imposed

by the interface was shown to lead to diminished screening of the ionic self-energy, resulting in an additional repulsion from the GDS. Levin & Flores-Mena's theory was shown to be in excellent agreement with experimental surface-tension data for NaCl solutions up to 1-M concentrations. However, when the same theory was applied to NaI solution, it predicted a qualitatively incorrect behavior. Specifically, the surface tension of NaI was found to be larger than that of NaCl, which was contradicted by experiments. Some key component clearly was still missing from the complete description of the interfacial properties of electrolyte solutions.

PA-DCT: polarizable anion dielectric continuum theory

A clue to the missing component was provided by the polarizable FF simulations discussed above. The prediction that the populations of the large halides (Br^- and I^-) are enhanced at the interface versus the bulk contradicted the very basis of the Onsager-Samaras theory, and polarizability seemed to play a role in promoting ion adsorption to the interface. To understand why polarizability is so important to ionic solvation, one needs to compare the electrostatic self-energy of an ion in vacuum and in bulk water (77). The self-energy of an ion of charge q and radius a in vacuum is $U_v \approx q^2/2a$, whereas in water it is $U_w \approx q^2/2\varepsilon_w a$, where $\varepsilon_w \approx 80$ is the dielectric constant of water. To move an ion of radius $a \approx 2$ Å from water to air therefore requires $140\,k_BT$ of work. This huge energy cost will always favor ionic solvation in bulk water. Let us suppose, however, that we want to move an ion not all the way into the vapor phase, but only to the interface, so that half of it is still hydrated. The electrostatic work that is needed to bring a hard nonpolarizable ion from bulk electrolyte to the surface is approximately $20\,k_BT$ (78). This is much less than the work needed to move the ion into the vapor, but it is still so large that it makes it energetically improbable to find an ion located near the GDS.

Now let us consider a perfectly polarizable ion that can be modeled as a conducting spherical shell of radius a and charge q, which is free to distribute itself over the surface of the ion. To minimize the electrostatic energy as a polarizable ion moves across the dielectric interface, its surface charge redistributes, so as to remain mostly hydrated. The work required to bring a polarizable ion toward the interface is approximately 10 times smaller ($\approx 2k_BT$) than that for a nonpolarizable ion (37, 77). Still, from the point of view of electrostatics, the interfacial ion location is unfavorable. What then drives large, highly polarizable halogen ions toward the air-water interface? To answer this question, we must consider the energetics of ionic solvation. To move an ion from vacuum into bulk water, we must first create a cavity from which water molecules are excluded, and this is both entropically and energetically costly. MD simulations provide an estimate of the cavitational free energy, which for an ion of $a \approx 2$ Å turns out to be approximately $2.5k_BT$ (77). If the ion moves toward the surface, the cavitational free energy will decrease proportionately to the volume of the ion exposed to air. For hard, nonpolarizable ions, this is too small to overcome the electrostatic self-energy penalty of exposing ionic charge to vacuum. For soft, polarizable ions, the situation is quite different. For large halogens such as Br^- and I^-, the stabilization due to the cavitational energy competes against the electrostatic self-energy penalty, as the two are now very similar in magnitude. Furthermore, the larger the ion is, the larger is the cavitational incentive for it to move toward the surface and the smaller is the electrostatic self-energy penalty. This is the basic idea behind the polarizable anion dielectric continuum theory (PA-DCT) (37, 77).

The general picture that emerges from the PA-DCT is that, near the air-water or a general hydrophobic interface, anions can be divided into two categories: kosmotropes and chaotropes (79). Kosmotropes, such as F^- and Cl^-, remain hydrated and are repelled from the GDS, whereas large, highly polarizable chaotropes such as Br^- and I^- shed some of their hydration shell and become stabilized at the interface by the cavitational and polarization contributions to the free energy (**Figure 1**). The PA-DCT affords the PMF for ion interactions with the interface (77), from which it is possible to obtain ion distributions and, via integration of the Gibbs adsorption

isotherm, the surface tensions of various electrolyte solutions, which are found to be in excellent agreement with experimental data (37, 79).

DFT: density functional theory

Generalized gradient approximation (GGA): class of exchange-correlation functionals that includes the electron density and its gradient

Hofmeister series: ordered ranking of ions according to their influence on a wide variety of chemical and biological processes

6. AB INITIO MOLECULAR DYNAMICS

Ab initio or first-principles molecular dynamics (FPMD) simulations, in which the forces are computed from the electronic structure, typically determined by density functional theory (DFT), are being increasingly applied to study ion behavior in interfacial settings. Until quite recently, the high computational cost of FPMD simulations limited their application in this area to ion-water clusters. For example, an FPMD simulation of a $Cl^-(H_2O)_6$ complex confirmed the surface location of the Cl^- ion predicted by FF-based simulations and provided insight into polarization effects and vibrational spectroscopy of the cluster (80). In 2004, Kuo & Mundy (81) pioneered the application of FPMD to an extended aqueous interface, specifically, an ≈35-Å-thick slab of 216 water molecules modeled with open interfaces in a $15 \times 15 \times 70$ Å cell with three-dimensional periodic boundary conditions. In addition to affording unprecedented detail into the structure, hydrogen bonding, and electronic structure of the air-water interface, Kuo & Mundy's simulation defined the protocols required to maintain a stable interface with a relatively small system and to obtain converged results for hydrogen bond populations and dynamics (82, 83).

FPMD simulations hold great potential to elucidate complex chemistry that can occur in the vicinity of aqueous interfaces, but this potential can only be realized if the underlying electronic structure method is sufficiently accurate. Kuo & Mundy's simulation of the air-water interface exposed additional weaknesses in a generalized gradient approximation (GGA) exchange-correlation functional, specifically, the BLYP functional, that was commonly used for aqueous systems. One problem that was immediately evident was that the equilibrium density of liquid water at ambient conditions was ≈0.8 g cc^{-1}, i.e., significantly less than the experimental value of 1 g cc^{-1}. This is a serious shortcoming because, without a proper bulk reference state, PMFs quantifying interfacial propensity are questionable.

Nevertheless, the simulation protocols established by Kuo & Mundy have been used in studies of the free energetics of adsorption of F^- and ClO_4^- anions at the air-water interface. Despite the issue with the bulk density, excellent qualitative agreement with experimentally inferred interfacial propensities, which follow the Hofmeister series (84), was obtained. Specifically, F^- was found to be strongly repelled from the interface, whereas ClO_4^- had a high interfacial propensity (64, 85). For a strongly hydrated ion such as F^-, it is likely that the bulk density will not qualitatively affect the strong repulsion that an ion will feel at the air-water interface because the tight solvation structure is preserved even at a reduced density (86). However, problems were reported in the ClO_4^- study owing to the coupling of the anion to strong density fluctuations of the slab that were attributed to the incorrect bulk density (85). Artifacts due to the incorrect bulk density have also been noticed in the solvation of OH^- (87).

Recent FPMD studies have sought to fix one well-known deficiency, namely, the lack of dispersion, and this area of research has already had a major impact on the protocol for DFT-based simulations of aqueous interfaces. With the inclusion of an empirical correction for dispersion due to Grimme (88), researchers showed that the density of liquid water utilizing GGA functionals is very close to 1 g cc^{-1} when simulated under constant temperature and pressure conditions (NPT ensemble) (89). As expected, these results carried over to extended slabs, in which excellent agreement with the NPT simulations was obtained (87, 90). Dispersion corrections also led to an improvement in other liquid water properties that were problematic previously, such as diffusion coefficients and radial distribution functions (87). The extent to which other equilibrium properties are affected by the addition of dispersion is presently an active line of inquiry. Obviously, this

simple extension of DFT cannot be expected to correct all the known problems, but it does provide a more solid platform for launching new DFT-based simulation studies of complex phenomena at aqueous interfaces.

The use of DFT for the study of bulk aqueous systems is not without controversy. Issues such as slow diffusion and overstructuring of bulk aqueous systems have led to some skepticism. Additional experimental tests of DFT are highly desirable, and a couple of recent examples have yielded encouraging results. Modern applications of multiedge X-ray absorption fine-structure (EXAFS) techniques have allowed researchers to precisely determine local structure through the assignment of multiple scattering paths (91, 92). Two recent FPMD studies of I^- and IO_3^- solvation have highlighted the importance of an ab initio representation of the interaction potential to describe the solvation structure (93, 94). In the case of I^-, a head-to-head comparison of a high-quality empirical polarizable potential to DFT revealed measurable differences in the first solvation shell (93). Although the differences were subtle, they came into full relief when examining the statistics of hydrogen bonding. The differences between the two interaction potentials were traced to a larger induced dipole for the polarizable model (by a factor of two), which was also noted in an independent investigation (95). This additional asymmetry under bulk solvation may have implications for surface propensity as well (96). The study of IO_3^- revealed a surprising and novel solvation structure in which the iodine center takes on a partial positive charge under bulk solvation and strongly coordinates three water molecules, whereas the negative partial charges on the oxygen atoms remain weakly hydrated (97). It was proposed that the strongly hydrated iodine atom is responsible for the surprising classification of IO_3^- as a kosmotrope, in agreement with the Jones-Dole *B* coefficient based on viscosity studies of electrolytes. It would be a challenge to describe the complex solvation of IO_3^- revealed by DFT accurately with empirical potentials.

The favorable comparison to EXAFS data has established that FPMD simulations with dispersion corrections can reproduce subtle details of the solvent shell accurately (93, 97). The same DFT approach was used recently to calculate the PMF for I^- adsorption at the air-water interface (94). Consistent with early studies that predicted I^- adsorption using polarizable FFs (22, 24, 25), the DFT PMF displays a local minimum at the interface (**Figure 2**). However, the minimum is much shallower than polarizable FFs predict and actually resembles PMFs obtained from nonpolarizable FFs more closely (42). Let us recall that the latter, when used in extended PB calculations, show reasonable agreement with surface-tension data. The shallow DFT PMF is also strikingly similar to the result from the PA-DCT (**Figure 2**), which reproduces experimental surface-tension and surface potential data remarkably well (76).

The similarity of the PMFs obtained using DFT, nonpolarizable FFs, and the PA-DCT is intriguing, and it raises a number of questions concerning the physics required to describe ion adsorption correctly. A priori it is safe to say that the physics contained in DFT is the most complete, but residual inaccuracies in the functionals and relatively very limited sampling (i.e., compared to FF-based MD simulations) are causes for concern that need to be addressed in future studies. Although it is encouraging that the extended PB calculations and the PA-DCT reproduce thermodynamic data for ion adsorption, it is not obvious why the single-ion PMF used in the former, which is derived from a nonpolarizable FF-based MD simulation (42), is so similar to the PMF for the latter, which is obtained via a DCT for polarizable anions (76).

EXAFS: extended X-ray absorption fine structure

Surface potential: electric potential difference across an interface that arises from broken symmetry

7. DRIVING FORCES FOR ION ADSORPTION

As evidence continues to mount from both simulations and experiments that certain ions have a propensity to adsorb at the air-water interface, the discussion has turned away from the question of whether ions adsorb and has moved toward the question of what the driving forces are for ion

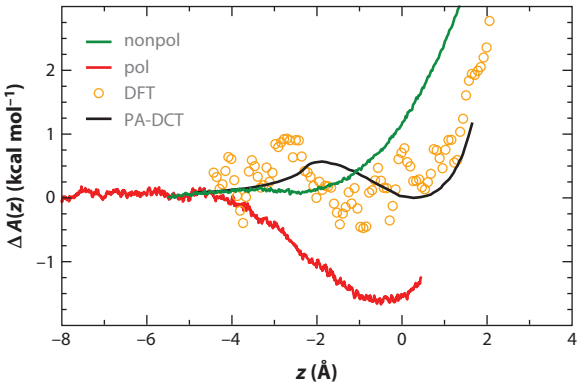

Figure 2

Comparisons of the potentials of mean force for I^- adsorption at the air-water interface (equivalent to the change in Helmholtz free energy accompanying the transfer of the ion from the middle of the water slab to a position z in the direction normal to the interface). The interface (Gibbs dividing surface) is located at $z = 0$. The black curve is from the polarizable anion dielectric continuum theory (PA-DCT) (37), the orange curve from density functional theory (DFT)-based first-principles molecular dynamics (MD) simulations (94), the red curve from an MD simulation using an empirical, polarizable potential (24), and the green curve from an MD simulation using an empirical, nonpolarizable potential (42).

adsorption. In light of the wealth of experimental and computational data, it seems that a consensus on the answer to this question ought to be on the horizon, yet recent theoretical studies have come to quite different conclusions. In the earliest simulation studies that employed polarizable empirical FFs, electronic polarization and ion size were identified as having an important influence on the propensity for anions to adsorb to extended aqueous interfaces (43). Until recently, it was assumed that ion adsorption is opposed by electrostatics, but that induction effects could reduce the electrostatic penalty, and is favored by hydrophobic/cavitational forces (44, 98). More recent studies, reviewed briefly below, have carefully evaluated these contributions and others, including the relative importance of ion-water and water-water interactions, local solvation effects, and the surface potential. The starting point for most analyses of driving forces for ion adsorption is the single-ion PMF, which is either decomposed into enthalpic and entropic components that are further dissected (99–102) or partitioned into free energy components (103, 104).

In the first approach, the entropic contribution to the free energy $-T\,\Delta S(z)$ is determined by subtracting the enthalpic contribution, which is essentially the average potential energy (assuming the PV term is negligible), $\langle \Delta U\,(z) \rangle$, from the PMF, $\Delta A(z)$, where z is a coordinate defining the position of the ion in the slab, and the Δ denotes a difference with respect to the bulk reference state. Assuming that the temperature dependence of the free energy of adsorption can be measured, all these quantities are accessible experimentally. Caleman et al. (101) recently reported a thermodynamic decomposition of single–halide ion PMFs, computed using MD simulations with polarizable FFs in large water clusters, into enthalpic and entropic contributions. Contrary to previous assumptions, they found that the adsorption of the heavier halides is favored by enthalpy and opposed by entropy. Otten et al. (102) came to the same conclusion based on simulations of fractionally charged iodide-like anions. They also employed resonant ultraviolet SHG spectroscopy to measure the adsorption of thiocyanate ions to the interface as a function of temperature (102). Fitting the SHG response to a Langmuir adsorption model allowed them to obtain changes in free energy, enthalpy, and entropy for the adsorptive process. The experimental results confirmed the simulation results, namely, that the negative free energy of adsorption of

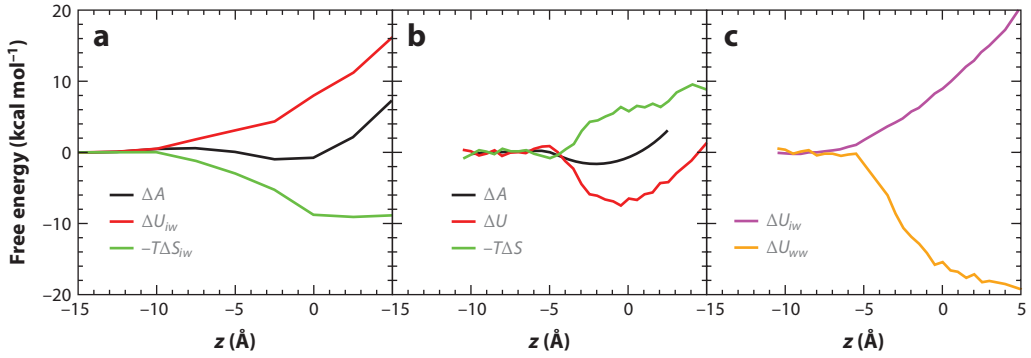

Figure 3

Thermodynamic decompositions of potentials of mean force for I^- adsorption computed from molecular dynamics simulations with polarizable force fields. The interface (Gibbs dividing surface) is located at $z = 0$. (*a*) Decomposition into ion-water enthalpy, ΔU_{iw}, and entropy, ΔS_{iw}, by Yagasaki et al. (108). (*b*) Decomposition into the total enthalpy, ΔU, and total entropy, ΔS, by Caleman et al. (101). (*c*) Decomposition of the enthalpy into ion-water and water-water contributions, ΔU_{iw} and ΔU_{ww}, respectively, by Caleman et al. (101).

the chaotropic SCN^- anion to the air-water interface is a consequence of the negative enthalpy of adsorption dominating the negative entropy of adsorption.

The enthalpy and entropy can be further decomposed into contributions from ion-water and water-water interactions. Although the meaning of the individual terms in the enthalpic decomposition is clear, that of the entropic terms is not. Several authors have asserted that a solvent-solvent contribution to the solvation entropy, attributed to the reorganization of the solvent in the presence of a solute, is exactly cancelled by the solvent-solvent contribution to the enthalpy, i.e., the change in the solvent-solvent interaction energy that accompanies the insertion of a solute into the solvent (see, e.g., 105–107). In this case, the solvation free energy of a single ion in neat water contains only contributions from changes in the ion-water interaction energy and an ion-water contribution to the entropy whose physical meaning is not clear. In other words, changes in water-water interactions do not contribute to the solvation free energy and hence do not constitute a driving force for solvation. In this vein, Yagasaki et al. (108) decomposed single–halide ion PMFs, computed from both polarizable and nonpolarizable FF-based simulations and quantum mechanics/molecular mechanics simulations in which the ions and their first solvent shell were modeled using Hartree-Fock theory with a 6-31G* basis set, into ion-water contributions to the enthalpy and entropy, the latter obtained as the difference between the free energy and the ion-water contribution to the enthalpy. They found that, for all the models of all the ions considered (F^-, Cl^-, and I^-), ion adsorption is opposed by the ion-water contribution to the enthalpy, as expected, and favored by the contribution to the PMF from the ion-water entropy (**Figure 3**). Yagasaki et al. also found that polarization contributes to stabilizing the interfacial location of the heavier halides, presumably by delaying the enthalpic cost of exposing the charge to vacuum.

A quite different set of conclusions emerges when the water-water contributions to the enthalpy are kept in the picture. Let us recall that both Caleman et al. (101) and Otten et al. (102) determined that the total enthalpy of adsorption is negative for halide and halide-like anions. Furthermore, they decomposed the enthalpy into ion-water and water-water contributions and found that the positive ion-water contribution (due to desolvation) is more than compensated by a negative contribution from water-water interactions (**Figure 3**). Thus they singled out changes in water-water interactions as a driving force for ion adsorption. Otten et al. (102) proceeded to show that water-water interactions are less favorable in the first solvation shell of the ion and at the

Quantum mechanics/molecular mechanics: hybrid simulation technique in which one region is treated quantum mechanically while the rest of the system is modeled with molecular mechanics

air-water interface than they are in bulk water and that, as an anion approaches the interface, it sheds some of its solvation shell and displaces water from the interface into the bulk. The negative water-water contribution to the adsorption enthalpy results therefore from a loss of less favorable hydration shell and surface water-water interactions, and an increase in more favorable water-water interactions. The authors concluded that the enthalpic driving force for ion adsorption arises from local changes in solvation.

Otten et al. (102) examined two possible explanations for the negative adsorption entropy. First, a change of the orientational statistics of water molecules in the ion hydration shell led to an estimate of the adsorption entropy that erred both in sign and magnitude from the value extracted from the temperature dependence of SHG data. Second, a reduction of entropy due to pinning of capillary waves by an ion at the interface, estimated by applying a harmonic model to the interfacial height fluctuations, led to a value that had the correct sign and was within a factor of two of the experimental value for the adsorption entropy.

Rather than focusing on enthalpic and entropic contributions to the free energy, Arslanargin & Beck (103) used a free energy partitioning approach to identify the predominant driving forces for anion adsorption. According to their analysis, the stabilization of a nonpolarizable iodide anion at the air-water interface results primarily from the reduction of the size of the cavity in water that accompanies adsorption and a far-field electrostatic contribution corresponding to the ion interaction with the interfacial surface potential. Around the same time, Baer et al. (104) came to a similar conclusion and showed that anion adsorption free energies obtained from MD simulations could be accurately reproduced by a DCT that includes free energy terms for cavity formation, electrostatic self-energy, and a modest electrochemical surface potential (≈ -0.3 V, which is about half the value of the surface potential of the water model used in the MD simulations).

The electric potential difference across the air-water interface arises because of the net orientation of water molecules in the interfacial region (13, 109). Surface potentials computed from MD simulations of point-charge water models tend to be approximately -0.5 V, and the analyses summarized above agree that the surface potential can be considered as a significant driving force for anion adsorption. The role of the surface potential becomes less clear, however, when results from FPMD simulations and the PA-DCT are included in the discussion. The PMF for iodide adsorption derived from the PA-DCT does not include a surface potential term, yet it agrees remarkably well with the iodide PMF computed from FPMD simulations (**Figure 2**) and reproduces experimental surface tension accurately (37). This juxtaposition of results suggests that the electrochemical surface potential felt by an adsorbing ion is negligible. However, the surface potential calculated explicitly from FPMD simulations is large and positive (110) and therefore should strongly oppose anion adsorption. This is not what is observed, e.g., in the PMF for I^- adsorption (94) (**Figure 2**), and reconciling this discrepancy is a subject of current research.

8. SOLUTIONS CONTAINING MIXTURES OF SALTS

Although much has been learned about the distributions of ions near atmospherically relevant aqueous interfaces by studying single-component electrolyte solutions, aqueous solutions in the atmosphere are multicomponent systems. For example, whereas the most prevalent ions in seawater are sodium cations and chloride anions, seawater also contains appreciable amounts of sulfate dianions and magnesium dications (111). Bromide anions, although present in seawater in only trace amounts ($\approx$1/600 the chloride concentration), are important because they play a major role in the chemistry of sea-salt aerosol (112, 113). Reactions of gaseous nitrogen oxides with halides in sea-salt aerosols leave behind nitrate anions, which can participate in photochemical reactions (10). For a complete description of the heterogeneous chemistry of aqueous ionic solutions in the

atmosphere, it is necessary to understand how the distribution of one species is affected by the presence of others. This issue has been addressed in several recent MD simulation and experimental studies.

Troposphere: region of the atmosphere between ground level and approximately 15-km altitude

Bromide enhancement at the air-water interface has been proposed to explain its high reactivity in sea-salt aerosols and on snow (9, 10, 14). In the first MD simulations of systems containing more than one polarizable halide, Jungwirth & Tobias (23) found that, in equimolar mixtures, chloride and bromide behaved as they did in single-component solutions at a low concentration (0.3 M), but at a higher concentration (3.0 M), the interfacial population of bromide was strongly enhanced, and chloride ions were pushed into the bulk. Two subsequent studies employed a combination of PES and MD simulations to further explore ion surface propensities in solutions of chloride/bromide mixtures. Ghosal et al. (114) obtained PES data on deliquesced and dissolved NaCl crystals doped with 7% or 10% Br^- and found that, in each case, the Br^-:Cl^- ratio was greater at the solution interface compared with that in the parent crystal. In the case of the crystal containing 7% Br^-, they were also able to show that the Cl^-:Na^+ ratio was significantly reduced (by ≈50%) at the surface of the solution versus the crystal. The ion distributions derived from a simulation of a mixed NaCl/NaBr solution containing 10% Br^-, and employing a polarizable FF, agreed qualitatively with the PES data. The simulation actually underpredicted the surface enhancement of Br^-, and the discrepancy was attributed to differences in the total ion concentrations in the simulation and experiment, as well as uncertainties in converting the spatial distributions from the simulations to distributions as a function of PKE for direct comparison to the PES data. Ottosson et al. (115) also used PES and MD simulations to determine ion distributions in solutions containing mixtures of Cl^- and Br^- and came to similar conclusions as the previous studies, namely, that Br^- is more surface enhanced in the mixtures versus in a neat solution of Br^- at a given concentration; i.e., NaCl salts out Br^- to the surface, and this effect increases with concentration. The preference of Cl^- for the interior and Br^- for the surface of the solution was rationalized in terms of the stronger hydration of Cl^- versus Br^-. A conclusion common to all the studies of Cl^-/Br^- mixtures is that, at high ion concentration, the behavior of individual ions in mixed-salt solutions cannot be extrapolated from their behavior in neat solutions of a single salt.

In light of the recent appreciation of the importance of iodine in halogen chemistry and particle formation in coastal environments (116, 117), Gladich et al. (118) performed an MD simulation study of solutions of ternary mixtures of NaCl, NaBr, and NaI modeled with a polarizable FF. In an equimolar mixture of the three components, the anion surface propensity followed the expected order: $Cl^- < Br^- < I^-$. Whereas increasing the concentration of Br^- (keeping the total ion concentration constant) did not result in changes of the surface propensity, increasing the concentration of Cl^- led to strong surface segregation of Br^- and I^-. Thus, consistent with simulations of Cl^-/Br^- mixtures, Cl^- was observed to salt out the heavier halides in the ternary mixtures. In a control simulation of the equimolar mixture with a nonpolarizable FF, all the ions behaved the same: None adsorbed to the interface; rather all remained well solvated in the interior of the solution, again underscoring the profound role that polarization plays in driving ion adsorption in MD simulations.

Nitrate is one of the most abundant inorganic aerosol components in both the remote and polluted troposphere (119). Nitrate photolysis is a source of OH (120, 121), the most important oxidant in the atmosphere (119). Whereas the quantum yield for nitrate photolysis in bulk solution is very low (≈0.06) (121), it appears that it is increased dramatically owing to a reduced solvent cage near the air-water interface (5, 6). Simulations have predicted that in neat nitrate solutions, although the nitrate anion makes occasional excursions to the air-water interface at which it is undercoordinated, it has on average a relatively low intrinsic interfacial propensity (e.g., as compared to the heavier halide anions) in large clusters and at extended aqueous surfaces

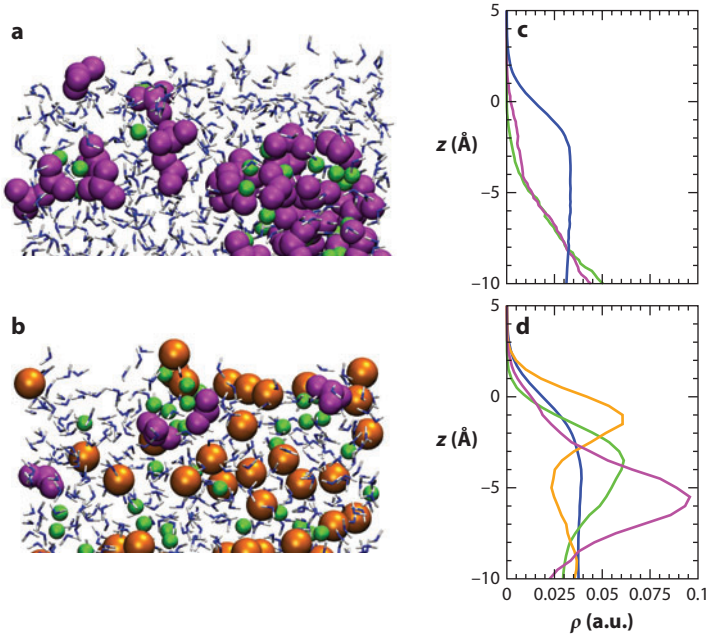

Figure 4

(*a*) Snapshot and (*b*) density profiles from a molecular dynamics (MD) simulation of 4-M $NaNO_3$ (aq) (6). Both the Na^+ and NO_3^- ions are for the most part repelled from the air-water interface ($z = 0$). NO_3^- ions are depicted with purple spheres, Na^+ ions as green spheres, Br^- ions as orange spheres, and water molecules as blue (oxygen atoms) and gray (hydrogen atoms) licorice. (*c*) Snapshot and (*d*) density profiles from an MD simulation of a 4-M mixture of $NaNO_3$ and NaBr (aq) with a mole fraction of NaBr equal to 0.9 (6). The NO_3^- density is enhanced below the double layer formed by adsorbed Br^- anions and Na^+ counterions. The colors of the curves in panels *c* and *d* correspond to the atom coloring in panels *a* and *b*.

(122–125). These predictions have been confirmed by SHG and PES experiments (126, 127). However, in more realistic models of sea-salt aerosol that contain mixtures of sodium nitrate and sodium halide salts, experiments have shown that the number of NO_2 molecules (a photolysis product) produced per NO_3^- irradiated increased with the fraction of the halide ions in the solution (5, 6). MD simulations employing polarizable FFs suggested that the electrical double layers formed by adsorbed halides followed by an excess of Na^+ ions draw NO_3^- anions close to the solution surface at which they are less solvated, and hence have reduced solvent cages, than in neat $NaNO_3$ solutions. **Figure 4** shows how NO_3^- ions are drawn closer to the air-water interface when $NaNO_3$ is mixed with NaBr. This is another example in which the behavior of ions in mixed-salt solutions cannot be inferred from their behavior in neat solutions.

Marine aerosols and inland aerosols originating from wind-blown dust contain a substantial amount of magnesium salts (10, 128); e.g., after NaCl, the next most abundant component of seawater is magnesium chloride, with one $MgCl_2$ molecule for every eight NaCl molecules (111). Mg^{2+} is unusual in that it does not form ion pairs with Cl^- in aqueous solution, even at high salt concentration (129). In two recent studies, Allen and coworkers (129, 130) used a combination of MD simulations and vibrational spectroscopy to investigate whether the unique solvation of Mg^{2+} affects the distribution and solvation of Cl^- near the solution-air interface of neat $MgCl_2$ over a range of concentrations (1.1 M to 4.9 M) and a model seawater solution comprising 4.5-M NaCl and 0.3-M $MgCl_2$. Even though magnesium remains well hydrated and has a strong influence

on the bulk structure of its solutions, they found that its presence does not have an appreciable effect on the distribution of chloride near the solution-air interface. However, they noted that the presence of Mg^{2+} does affect the microsolvation of chloride in the interfacial region, and they suggested that this could in turn affect its heterogeneous reactivity.

9. SUMMARY AND OUTLOOK

A little over a decade ago, MD simulations became established as a useful approach to gain molecular-scale information on chemistry occurring at aqueous interfaces in the atmosphere. MD simulations exposed some unexpected behavior of reactive ions near the air-water interface, namely, that some ions adsorb, contrary to longstanding conventional wisdom. Simulation studies are helping to elucidate the driving forces for ion adsorption and are paving the way for new developments in theory, such as the PA-DCT reviewed here. FPMD simulations have begun to provide unprecedented details on the solvation of ions in bulk and interfacial settings and have started to be applied to study chemical reactions involving ions and acids that are important in atmospheric chemistry (see, e.g., 131–135). Although this review stresses the relevance of the behavior of ions at aqueous solution-air interfaces to atmospheric chemistry, the discoveries reviewed here have led to new concepts that are much more widely applicable, e.g., to the broad spectrum of specific ion effects commonly referred to as Hofmeister effects.

SUMMARY POINTS

1. FF-based MD simulations and, increasingly, DFT-based MD simulations are providing atomic-scale insight into the structure and reactivity of aqueous interfaces in the atmosphere.
2. To make progress in the validation of FFs used to model aqueous ionic solutions, investigators need to reconcile the little or no adsorption inferred from surface-tension data with the relatively strong adsorption implied by most available spectroscopic data.
3. The PA-DCT affords the PMF for ion interactions with the interface, from which it is possible to obtain ion distributions and, via integration of the Gibbs adsorption isotherm, the surface tensions of various electrolyte solutions, which are found to be in excellent agreement with experimental data.
4. Recent studies have carefully evaluated the driving forces that have been identified as having an important influence on the propensity for anions to adsorb to extended aqueous interfaces. There is still considerable debate regarding the relative importance of induction effects, cavitation, ion-water and water-water interactions, local solvation effects, and the surface potential.
5. The role of the surface potential in promoting or opposing ion adsorption in point-charge models of the air-water interface is beginning to be understood, but its role in ab initio models of the interface, for which the surface potential has the opposite sign and is an order of magnitude larger, is not yet clear.
6. The behavior of ions in concentrated mixed-salt solutions cannot be inferred from their behavior in neat solutions. Examples include the formation of electrical double layers by adsorbed halides and their counterions, and the enhanced interfacial population of Br^- in concentrated NaCl solutions.

DISCLOSURE STATEMENT

The authors are not aware of any affiliations, memberships, funding, or financial holdings that might be perceived as affecting the objectivity of this review.

ACKNOWLEDGMENTS

A.C.S. and D.J.T. are grateful for support from the AirUCI collaborative, which is funded by the National Science Foundation (grant CHE-0431312). M.D.B. and C.J.M. acknowledge support from the US Department of Energy's Office of Basic Energy Sciences, Division of Chemical Sciences, Geosciences, and Biosciences. Pacific Northwest National Laboratory (PNNL) is operated for the Department of Energy by Battelle. M.D.B. is supported by the Linus Pauling Distinguished Postdoctoral Fellowship Program at PNNL. Y.L. acknowledges partial support by the CNPq, FAPERGS, INCT-FCx, and the US-AFOSR (grant FA9550-09-1-0283). We are grateful to Dr. Karen Callahan for assistance in the preparation of **Figure 4**.

LITERATURE CITED

1. Hu JH, Shi Q, Davidovits P, Worsnop DR, Zahniser MS, Kolb CE. 1995. Reactive uptake of Cl_2 (g) and Br_2 (g) by aqueous surfaces as a function of Br^- and I^- ion concentration: the effect of chemical reaction at the interface. *J. Phys. Chem.* 99:8768–76
2. Knipping EM, Lakin MJ, Foster KL, Jungwirth P, Tobias DJ, et al. 2000. Experiments and simulations of ion-enhanced interfacial chemistry on aqueous NaCl aerosols. *Science* 288:301–6
3. Hunt SW, Roeselova M, Wang W, Wingen LM, Knipping EM, et al. 2004. Formation of molecular bromine from the reaction of ozone with deliquesced NaBr aerosol: evidence for interface chemistry. *J. Phys. Chem. A* 108:11559–72
4. Clifford D, Donaldson DJ. 2007. Direct experimental evidence for a heterogeneous reaction of ozone with bromide at the air-aqueous interface. *J. Phys. Chem. A* 111:9809–14
5. Wingen LM, Moskun AC, Johnson SN, Thomas JL, Roeselova M, et al. 2008. Enhanced surface photochemistry in chloride-nitrate ion mixtures. *Phys. Chem. Chem. Phys.* 10:5668–77
6. Richards NK, Wingen LM, Callahan KM, Nishino N, Kleinman MT, et al. 2011. Nitrate ion photolysis in thin water films in the presence of bromide ions. *J. Phys. Chem. A* 115:5810–21
7. Calvert JG, Lazrus A, Kok GL, Heikes BG, Walega JG, et al. 1985. Chemical mechanisms of acid generation in the troposphere. *Nature* 317:27–35
8. Knipping EM, Dabdub D. 2003. Impact of chlorine emissions from sea-salt aerosol on coastal urban ozone. *Environ. Sci. Technol.* 37:275–84
9. Simpson WR, von Glasow R, Riedel K, Anderson P, Ariya P, et al. 2007. Halogens and their role in polar boundary-layer ozone depletion. *Atmos. Chem. Phys.* 7:4375–418
10. Finlayson-Pitts BJ. 2009. Reactions at surfaces in the atmosphere: integration of experiments and theory as necessary (but not necessarily sufficient) for predicting the physical chemistry of aerosols. *Phys. Chem. Chem. Phys.* 11:7760–79
11. Jungwirth P, Tobias DJ. 2006. Specific ion effects at the air/water interface. *Chem. Rev.* 106:1259–81
12. Gerber RB, Sebek J. 2009. Dynamics simulations of atmospherically relevant molecular reactions. *Int. Rev. Phys. Chem.* 28:207–22
13. Netz RR, Horinek D. 2012. Progress in modeling of ion effects at the vapor/water interface. *Annu. Rev. Phys. Chem.* 63:401–18
14. Finlayson-Pitts BJ. 2010. Halogens in the troposphere. *Anal. Chem.* 82:770–76
15. Perera L, Berkowitz ML. 1991. Many-body effects in molecular dynamics simulations of Na^+ $(H_2O)_n$ and Cl^- $(H_2O)_n$ clusters. *J. Chem. Phys.* 95:1954–63
16. Perera L, Berkowitz ML. 1992. Structure and dynamics of Cl^- $(H_2O)_{20}$ clusters: the effect of the polarizability and the charge of the ion. *J. Chem. Phys.* 96:8288–94

17. Perera L, Berkowitz ML. 1993. Stabilization energies of Cl^-, Br^-, and I^- ions in water clusters. *J. Chem. Phys.* 99:4222–24
18. Caldwell J, Dang LX, Kollman PA. 1990. Implementation of nonadditive intermolecular potentials by use of molecular dynamics: development of a water-water potential and water-ion cluster interactions. *J. Am. Chem. Soc.* 112:9144–47
19. Dang LX, Smith DE. 1993. Molecular dynamics simulations of aqueous ionic clusters using polarizable water. *J. Chem. Phys.* 99:6950–56
20. Stuart SJ, Berne BJ. 1996. Effects of polarizability on the hydration of the chloride ion. *J. Phys. Chem.* 100:11934–43
21. Stuart SJ, Berne BJ. 1999. Surface curvature effects in the aqueous ionic solvation of the chloride ion. *J. Phys. Chem. A* 103:10300–7
22. Jungwirth P, Tobias DJ. 2001. Molecular structure of salt solutions: a new view of the interface with implications for heterogeneous atmospheric chemistry. *J. Phys. Chem. B* 105:10468–72
23. Jungwirth P, Tobias DJ. 2002. Ions at the air/water interface. *J. Phys. Chem. B* 106:6361–73
24. Dang LX. 2002. Computational study of ion binding to the liquid interface of water. *J. Phys. Chem. B* 106:10388–94
25. Dang LX, Chang T-M. 2002. Molecular mechanism of ion binding to the liquid/vapor interface of water. *J. Phys. Chem. B* 106:235–38
26. Petersen PB, Saykally RJ. 2004. Confirmation of enhanced anion concentration at the liquid water surface. *Chem. Phys. Lett.* 397:51–55
27. Petersen PB, Johnson JC, Knutsen KP, Saykally RJ. 2004. Direct experimental validation of the Jones-Ray effect. *Chem. Phys. Lett.* 397:46–50
28. Petersen PB, Saykally RJ. 2006. Probing the interfacial structure of aqueous electrolytes with femtosecond second harmonic generation spectroscopy. *J. Phys. Chem. B* 110:14060–73
29. Liu D, Ma G, Levering LM, Allen HC. 2004. Vibrational spectroscopy of aqueous sodium halide solutions and air-liquid interfaces: observation of increased interfacial depth. *J. Phys. Chem. B* 108:2252–60
30. Raymond EA, Richmond GL. 2004. Probing the molecular structure and bonding of the surface of aqueous salt solutions. *J. Phys. Chem. B* 108:5051–59
31. Winter B, Weber R, Schmidt PM, Hertel IV, Faubel M, et al. 2004. Molecular structure of surface-active salt solutions: photoelectron spectroscopy and molecular dynamics simulations of aqueous tetrabutylammonium iodide. *J. Phys. Chem. B* 108:14558–64
32. Ghosal S, Hemminger JC, Bluhm H, Mun BS, Hebenstreit ELD, et al. 2005. Electron spectroscopy of aqueous solution interfaces reveals surface enhancement of halides. *Science* 307:563–66
33. Gopalakrishnan S, Liu D, Allen HC, Kuo M, Shultz MJ. 2006. Vibrational spectroscopic studies of aqueous interfaces: salts, acids, bases, and nanodrops. *Chem. Rev.* 106:1155–75
34. Winter B, Faubel M. 2006. Photoemission from liquid aqueous solutions. *Chem. Rev.* 106:1176–211
35. Chang T-M, Dang LX. 2006. Recent advances in molecular simulations of ion solvation at liquid interfaces. *Chem. Rev.* 106:1305–22
36. Petersen PB, Saykally RJ. 2006. On the nature of ions at the liquid water surface. *Annu. Rev. Phys. Chem.* 57:333–64
37. Levin Y, dos Santos AP, Diehl A. 2009. Ions at the air-water interface: an end to a hundred-year-old mystery? *Phys. Rev. Lett.* 103:257802
38. Grossfield A, Ren P, Ponder JW. 2003. Ion solvation thermodynamics from simulation with a polarizable force field. *J. Am. Chem. Soc.* 125:15671–82
39. Yu H, Whitfield TW, Harder E, Lamoureux G, Vorobyov I, et al. 2010. Simulating monovalent and divalent ions in aqueous solution using a Drude polarizable force field. *J. Chem. Theory Comput.* 6:774–86
40. Warren GL, Patel S. 2008. Comparison of the solvation structure of polarizable and nonpolarizable ions in bulk water and near the aqueous liquid-vapor interface. *J. Phys. Chem. C* 112:7455–67
41. Horinek D, Mamatkulov SI, Netz RR. 2009. Rational design of ion force fields based on thermodynamic solvation properties. *J. Chem. Phys.* 130:124507

22. Presents a pioneering MD simulation study of ion distributions at extended sodium halide solution-air interfaces.

26. Provides the first verification of the enhanced concentration of anions at the solution interface by SHG.

29. Revealed for the first time the perturbation of interfacial water hydrogen bonding by bromide and iodide anions using VSFG.

32. Measures the composition of the liquid/vapor interface using X-ray PES.

42. Horinek D, Herz A, Vrbka L, Sedlmeir F, Mamatkulov SI, Netz RR. 2009. Specific ion adsorption at the air/water interface: the role of hydrophobic solvation. *Chem. Phys. Lett.* 479:173–83
43. Vrbka L, Mucha M, Minofar B, Jungwirth P, Brown EC, Tobias DJ. 2004. Propensity of soft ions for the air/water interface. *Curr. Opin. Colloid Interface Sci.* 9:67–73
44. Noah-Vanhoucke J, Geissler PL. 2009. On the fluctuations that drive small ions toward, and away from, interfaces between polar liquids and their vapors. *Proc. Natl. Acad. Sci. USA* 106:15125–30
45. Eggimann BL, Siepmann JI. 2008. Size effects on the solvation of anions at the aqueous liquid-vapor interface. *J. Phys. Chem. C* 112:210–18
46. Heydweiller A. 1910. Concerning the physical characteristics of solutions in correlation. II. Surface tension and electronic conductivity of watery salt solutions. *Ann. Phys.* 33:145–85
47. Washburn EW. 1928. *International Critical Tables of Numerical Data. Physics, Chemistry, and Technology*, Vol. 4. New York: McGraw-Hill
48. dos Santos DJVA, Müller-Plathe F, Weiss VC. 2008. Consistency of ion adsorption and excess surface tension in molecular dynamics simulations of aqueous salt solutions. *J. Phys. Chem. C* 112:19431–42
49. D'Auria R, Tobias DJ. 2009. Relation between surface tension and ion adsorption at the air-water interface: a molecular dynamics simulation study. *J. Phys. Chem. A* 113:7286–93
50. Horinek D, Netz RR. 2007. Specific ion adsorption at hydrophobic solid surfaces. *Phys. Rev. Lett.* 99:226104
51. Richmond GL. 2002. Molecular bonding and interactions at aqueous surfaces as probed by vibrational sum frequency spectroscopy. *Chem. Rev.* 102:2693–724
52. Shen YR, Ostroverkhov V. 2006. Sum-frequency vibrational spectroscopy on water interfaces: polar orientation of water molecules at interfaces. *Chem. Rev.* 106:1140–54
53. Ji N, Ostroverkhov V, Chen CY, Shen YR. 2007. Phase-sensitive sum-frequency vibrational spectroscopy and its application to studies of interfacial alkyl chains. *J. Am. Chem. Soc.* 129:10056–57
54. Morita A, Hynes JT. 2002. A theoretical analysis of the sum frequency generation spectrum of the water surface. II. Time-dependent approach. *J. Phys. Chem. B* 106:673–85
55. Brown EC, Mucha M, Jungwirth P, Tobias DJ. 2005. Structure and vibrational spectroscopy of salt water/air interfaces: predictions from classical molecular dynamics simulations. *J. Phys. Chem. B* 109:7934–40
56. Buch V, Tarbuck T, Richmond GL, Groenzin H, Li I, Shultz MJ. 2007. Sum frequency generation surface spectra of ice, water, and acid solution investigated by an exciton model. *J. Chem. Phys.* 127:204710
57. Noah-Vanhoucke J, Smith JD, Geissler PL. 2009. Toward a simple molecular understanding of sum frequency generation at air-water interfaces. *J. Phys. Chem. B* 113:4065–74
58. Auer BM, Skinner JL. 2009. Vibrational sum-frequency spectroscopy of the water liquid/vapor interface. *J. Phys. Chem. B* 113:4125–30
59. Ishiyama T, Morita A. 2006. Intermolecular correlation effect in sum frequency generation spectroscopy of electrolyte aqueous solution. *Chem. Phys. Lett.* 431:78–82
60. Ishiyama T, Morita A. 2007. Molecular dynamics study of gas-liquid aqueous sodium halide interfaces. II. Analysis of vibrational sum frequency generation spectra. *J. Phys. Chem. C* 111:738–48
61. Onorato RM, Otten DE, Saykally RJ. 2010. Measurement of bromide ion affinities for the air/water and dodecanol/water interfaces at molar concentrations by UV second harmonic generation spectroscopy. *J. Phys. Chem. C* 114:13746–51
62. Bluhm H, Andersson K, Araki T, Benzerara K, Brown GE, et al. 2006. Soft X-ray microscopy and spectroscopy at the molecular environmental science beamline at the Advanced Light Source. *J. Electron Spectrosc. Relat. Phenom.* 150:86–104
63. Ottosson N, Faubel M, Bradforth SE, Jungwirth P, Winter B. 2010. Photoelectron spectroscopy of liquid water and aqueous solution: electron effective attenuation lengths and emission-angle anisotropy. *J. Electron Spectrosc. Relat. Phenom.* 177:60–70
64. Brown MA, D'Auria R, Kuo I-FW, Krisch MJ, Starr DE, et al. 2008. Ion spatial distributions at the liquid-vapor interface of aqueous potassium fluoride solutions. *Phys. Chem. Chem. Phys.* 10:4778–84
65. Cheng MH, Callahan KM, Margarella AM, Tobias DJ, Hemminger JC. 2012. Ambient pressure X-ray photoelectron spectroscopy and molecular dynamics simulation studies of liquid/vapor interfaces of aqueous NaCl, RbCl, and RbBr solutions. *J. Phys. Chem. C* 116:4545–55

66. Krisch MJ, D'Auria R, Brown MA, Tobias DJ, Hemminger JC, et al. 2007. The effect of an organic surfactant on the liquid-vapor interface of an electrolyte solution. *J. Phys. Chem. C* 111:13497–509
67. Sloutskin E, Baumert J, Ocko BM, Kuzmenko I, Checco A, et al. 2007. The surface structure of concentrated aqueous salt solutions. *J. Chem. Phys.* 126:054704
68. Sun X, Dang LX. 2009. Computational studies of aqueous interfaces of RbBr salt solutions. *J. Chem. Phys.* 130:124709
69. Sun X, Wick CD, Dang LX. 2009. Computational studies of aqueous interfaces of $SrCl_2$ salt solutions. *J. Phys. Chem. B* 113:13993–97
70. Dang LX, Sun X, Ginovska-Pangovska B, Annapureddy HVR, Truong TB. 2013. Understanding ion-ion interactions in bulk and aqueous interfaces using molecular simulations. *Faraday Discuss.* 160:151–60
71. Debye P, Hückel E. 1923. Lowering of freezing point and related phenomena. *Z. Phys.* 24:185–206
72. Levin Y. 2002. Electrostatic correlations: from plasma to biology. *Rep. Prog. Phys.* 65:1577–632
73. Langmuir I. 1917. The constitution and fundamental properties of solids and liquids. II. Liquids. *J. Am. Chem. Soc.* 39:1848–906
74. Wagner C. 1924. The surface tension of dilute solutions of electrolytes. *Phys. Z.* 25:474–77
75. Onsager L, Samaras NNT. 1934. The surface tension of Debye-Hückel electrolytes. *J. Chem. Phys.* 2:528–36
76. Levin Y, Flores-Mena JE. 2001. Surface tension of strong electrolytes. *Europhys. Lett.* 56:187–92
77. Levin Y. 2009. Polarizable ions at interfaces. *Phys. Rev. Lett.* 102:147803
78. Tamashiro MN, Constantino MA. 2010. Ions at the water-vapor interface. *J. Phys. Chem. B* 114:3583–91
79. dos Santos AP, Diehl A, Levin Y. 2010. Surface tensions, surface potentials, and the Hofmeister series of electrolyte solutions. *Langmuir* 26:10778–83
80. Tobias DJ, Jungwirth P, Parrinello M. 2001. Surface solvation of halogen anions in water clusters: an ab initio molecular dynamics study of the Cl^- $(H_2O)_6$ complex. *J. Chem. Phys.* 114:7036–44
81. Kuo I-FW, Mundy CJ. 2004. An ab initio molecular dynamics study of the aqueous liquid-vapor interface. *Science* 303:658–60
82. Mundy CJ, Kuo I-FW. 2006. First-principles approaches to the structure and reactivity of atmospherically relevant aqueous interfaces. *Chem. Rev.* 106:1282–304
83. Kuo I-FW, Mundy CJ, Eggimann BL, McGrath MJ, Siepmann JI, et al. 2006. Structure and dynamics of the aqueous liquid-vapor interface: a comprehensive particle-based simulation study. *J. Phys. Chem. B* 110:3738–46
84. Pegram LM, Record MT Jr. 2007. Hofmeister salt effects on surface tension arise from partitioning of anions and cations between bulk water and the air-water interface. *J. Phys. Chem. B* 111:5411–17
85. Baer MD, Kuo I-FW, Bluhm H, Ghosal S. 2009. Interfacial behavior of perchlorate versus chloride ions in aqueous solutions. *J. Phys. Chem. B* 113:15843–50
86. Ho MH, Klein ML, Kuo I-FW. 2009. Bulk and interfacial aqueous fluoride: an investigation via first principles molecular dynamics. *J. Phys. Chem. A* 113:2070–74
87. Baer MD, Mundy CJ, McGrath MJ, Siepmann JI, Tobias DJ. 2011. Re-examining the properties of the aqueous vapor-liquid interface using dispersion corrected density functional theory. *J. Chem. Phys.* 135:124712
88. Grimme S. 2006. Semiempirical GGA-type density functional constructed with long-range dispersion correction. *J. Comput. Chem.* 27:1787–99
89. Schmidt J, Vandevondele J, Kuo I-FW, Sebastiani D, Siepmann JI, et al. 2009. Isobaric-isothermal molecular dynamics simulations utilizing density functional theory: an assessment of the structure and density of water at near-ambient conditions. *J. Phys. Chem. B* 113:11959–64
90. Kühne TD, Pascal TA, Kaxiras E, Jung Y. 2011. New insights into the structure of the vapor/water interface from large-scale first-principles simulations. *J. Phys. Chem. Lett.* 2:105–13
91. McCarthy ML, Schenter GK, Chacon Taylor MR, Rehr JJ, Brown GE. 1997. Prediction of extended X-ray-absorption fine-structure spectra from molecular interaction models: Na^+ $(H_2O)_{(n)}$-MgO (100) interface. *Phys. Rev. B* 56:9925–36
92. Dang LX, Schenter GK, Glezakou VA, Fulton JL. 2006. Molecular simulation analysis and X-ray absorption measurement of Ca^{2+}, K^+, and Cl^- ions in solution. *J. Phys. Chem. B* 110:23644–54

77. Presents a PA-DCT that agrees well with experimental surface tension and surface potential data.

89. Shows that the Grimme empirical dispersion correction to DFT improves water density and structure in constant-pressure MD simulations.

93. Fulton JL, Schenter GK, Baer MD, Mundy CJ, Dang LX, Balasubramanian M. 2010. Probing the hydration structure of polarizable halides: a multiedge XAFS and molecular dynamics study of the iodide anion. *J. Phys. Chem. B* 114:12926–37

94. Computes the PMF of transferring an iodide from the bulk to an interface using DFT.

94. Baer MD, Mundy CJ. 2011. Towards an understanding of the specific ion effect using density functional theory. *J. Phys. Chem. Lett.* 2:1088–93

95. Beck TL. 2011. A local entropic signature of specific ion hydration. *J. Phys. Chem. B* 115:9776–81

96. Wick CD, Cummings OT. 2011. Understanding the factors that contribute to ion interfacial behavior. *Chem. Phys. Lett.* 513:161–66

97. Baer MD, Pham VT, Fulton JL, Schenter GK, Balasubramanian M, Mundy CJ. 2011. Is iodate a strongly hydrated cation? *J. Phys. Chem. Lett.* 2:2650–54

98. Archontis G, Leontidis E. 2006. Dissecting the stabilization of iodide at the air-water interface into components: a free energy analysis. *Chem. Phys. Lett.* 420:199–203

99. Herce DH, Perera L, Darden TA, Sagui C. 2005. Surface solvation for an ion in a water cluster. *J. Chem. Phys.* 122:024513

100. Yagasaki T, Saito S, Ohmine I. 2010. Effects of nonadditive interactions on ion solvation at the water/vapor interface: a molecular dynamics study. *J. Phys. Chem. A* 114:12573–84

101. Reports single–halide ion PMFs and their decomposition into enthalpic and entropic contributions.

101. Caleman C, Hub JS, van Maaren PJ, van der Spoel D. 2011. Atomistic simulation of ion solvation in water explains surface preference of halides. *Proc. Natl. Acad. Sci. USA* 108:6838–42

102. Demonstrates with ultraviolet SHG spectroscopy and simulations the enthalpic promotion and entropic opposition to anion adsorption.

102. Otten DE, Shaffer PR, Geissler PL, Saykally RJ. 2012. Elucidating the mechanism of selective ion adsorption to the liquid water surface. *Proc. Natl. Acad. Sci. USA* 109:701–5

103. Presents the decomposition of ion adsorption free energy into contributions from cavity formation, dispersion, and local and far-field electrostatics.

103. Arslanargin A, Beck TL. 2012. Free energy partitioning analysis of the driving forces that determine ion density profiles near the water liquid-vapor interface. *J. Chem. Phys.* 136:104503

104. Baer MD, Stern AC, Levin Y, Tobias DJ, Mundy CJ. 2012. Electrochemical surface potential due to classical point charge models drives anion adsorption to the air-water interface. *J. Phys. Chem. Lett.* 3:1565–70

105. Yu H-A, Karplus M. 1988. A thermodynamic analysis of solvation. *J. Chem. Phys.* 89:2366–79

106. Guillot B, Guissani Y. 1993. A computer simulation study of the temperature dependence of the hydrophobic hydration. *J. Chem. Phys.* 99:8075–94

107. Ben-Amotz D, Raineri F, Stell G. 2005. Solvation thermodynamics: theory and applications. *J. Phys. Chem. B* 109:6866–78

108. Yagasaki T, Saito S, Ohmine I. 2010. Effects of nonadditive interactions on ion solvation at the water/vapor interface: a molecular dynamics study. *J. Phys. Chem. A* 114:12573–84

109. Wilson M, Pohorille A, Pratt LR. 1988. Surface potential of the water liquid-vapor interface. *J. Chem. Phys.* 88:3281–85

110. Kathmann SM, Kuo I-FW, Mundy CJ, Schenter GK. 2011. Understanding the surface potential of water. *J. Phys. Chem. B* 115:4369–77

111. Lide DR. 1996. *CRC Handbook of Chemistry and Physics*. Boca Raton, FL: CRC

112. Finlayson-Pitts BJ, Hemminger JC. 2000. Physical chemistry of airborne sea salt particles and their components. *J. Phys. Chem. A* 104:11463–77

113. Finlayson-Pitts BJ. 2003. The tropospheric chemistry of sea salt: a molecular-level view of the chemistry of NaCl and NaBr. *Chem. Rev.* 103:4801–22

114. Ghosal S, Brown MA, Bluhm H, Krisch MJ, Salmeron M, et al. 2008. Ion partitioning at the liquid/vapor interface of a multicomponent alkali halide solution: a model for aqueous sea salt aerosols. *J. Phys. Chem. A* 112:12378–84

115. Ottosson N, Heyda J, Wernersson E, Pokapanich W, Svensson S, et al. 2010. The influence of concentration of the molecular surface structure of simple and mixed aqueous electrolytes. *Phys. Chem. Chem. Phys.* 12:10693–700

116. Saiz-Lopez A, Mahajan AS, Salmon RA, Bauguitte SJ-B, Jones AE, et al. 2007. Boundary layer halogens in coastal Antarctica. *Science* 317:348–51

117. Huang RJ, Seitz K, Neary T, O'Dowd CD, Platt U, Hoffmann T. 2010. Observations of high concentrations of I_2 and IO in coastal air supporting iodine-oxide driven coastal new particle formation. *Geophys. Res. Lett.* 37:L03803

118. Gladich I, Shepson PB, Carignano MA, Szleifer I. 2011. Halide affinity for the water-air interface in aqueous solutions of mixtures of sodium salts. *J. Phys. Chem. A* 115:5895–99
119. Finlayson-Pitts BJ, Pitts JN Jr. 2000. *Chemistry of the Upper and Lower Atmosphere: Theory, Experiments, and Applications*. San Diego: Academic
120. Mack J, Bolton JR. 1999. Photochemistry of nitrite and nitrate in aqueous solution: a review. *J. Photochem. Photobiol. A* 128:1–13
121. Herrmann H. 2007. On the photolysis of simple anions and neutral molecules as sources of O^-/OH, SOx^- and Cl in aqueous solution. *Phys. Chem. Chem. Phys.* 9:3935–64
122. Minofar B, Vacha R, Wahab A, Mahiuddin S, Kunz W, Jungwirth P. 2006. Propensity for the air/water interface and ion pairing in magnesium acetate versus magnesium nitrate solutions: molecular dynamics simulations and surface tension measurements. *J. Phys. Chem. B* 110:15939–44
123. Dang LX, Chang T-M, Roeselova M, Garrett BC, Tobias DJ. 2006. On $NO_3^- - H_2O$ interactions in aqueous solutions and at interfaces. *J. Chem. Phys.* 124:066101
124. Thomas JL, Roeselova M, Dang LX, Tobias DJ. 2007. Molecular dynamics simulations of the solution-air interface of aqueous sodium nitrate. *J. Phys. Chem. A* 111:3091–98
125. Miller Y, Thomas JL, Kemp DD, Finlayson-Pitts BJ, Tobias DJ, Gerber RB. 2009. Structure of large nitrate-water clusters at ambient temperatures: simulations with effective fragment potentials and force fields with implications for atmospheric chemistry. *J. Phys. Chem. A* 113:12805–14
126. Otten DE, Petersen PB, Saykally RJ. 2007. Observation of nitrate ions at the air/water interface by UV-second harmonic generation. *Chem. Phys. Lett.* 449:261–65
127. Brown MA, Winter B, Faubel M, Hemminger JC. 2009. Spatial distribution of nitrate and nitrite anions at the liquid/vapor interface of aqueous solutions. *J. Am. Chem. Soc.* 131:8355–56
128. Gill TE, Gillette DA, Niemeyer T, Winn RT. 2002. Elemental geochemistry of wind-erodible playa sediments, Owens Lake, California. *Nucl. Instrum. Methods B* 113:209–13
129. Callahan KM, Casillas-Ituarte NN, Xu M, Roeselova M, Allen HC, Tobias DJ. 2010. Effect of magnesium cation on the interfacial properties of aqueous salt solutions. *J. Phys. Chem. A* 114:8359–68
130. Casillas-Ituarte NN, Callahan KM, Tank CY, Chen X, Roeselova M, et al. 2010. Surface organization of aqueous $MgCl_2$ and application to atmospheric marine aerosol chemistry. *Proc. Natl. Acad. Sci. USA* 107:6616–21
131. Shamay ES, Buch V, Parrinello M, Richmond GL. 2007. At the water's edge: nitric acid as a weak acid. *J. Am. Chem. Soc.* 129:12910–11
132. Wang S, Bianco R, Hynes JT. 2009. Depth-dependent dissociation of nitric acid at an aqueous surface: Car-Parrinello molecular dynamics. *J. Phys. Chem. A* 113:1295–307
133. Lee H-S, Tuckerman ME. 2009. Ab initio molecular dynamics studies of the liquid-vapor interface of an HCl solution. *J. Phys. Chem. A* 113:2144–51
134. Lewis T, Winter B, Stern AC, Baer MD, Mundy CJ, et al. 2011. Does nitric acid dissociate at the aqueous solution surface? *J. Phys. Chem. C* 115:21183–90
135. Hammerich AD, Buch V. 2012. Ab initio molecular dynamics simulations of the liquid/vapor interface of sulfuric acid solutions. *J. Phys. Chem. A* 116:5637–52

Annual Review of
Physical Chemistry
Volume 64, 2013

Contents

Indexes

Errata

An online log of corrections to *Annual Review of Physical Chemistry* articles may be found at http://physchem.annualreviews.org/errata.shtml